Quantum critical temperature of a modulated oscillator

Lingzhen Guo,[1,2] Vittorio Peano,[3,*] M. Marthaler,[1,4] and M. I. Dykman[3]
[1]*Institut für Theoretische Festkörperphysik, Karlsruhe Institute of Technology, 76128 Karlsruhe, Germany*
[2]*Department of Physics, Beijing Normal University, Beijing 100875, China*
[3]*Department of Physics and Astronomy, Michigan State University, East Lansing, Michigan 48824, USA*
[4]*DFG Center for Functional Nanostructures (CFN), Karlsruhe Institute of Technology, 76128 Karlsruhe, Germany*
(Received 12 December 2012; published 24 June 2013)

We show that the rate of switching between the vibrational states of a modulated nonlinear oscillator is characterized by a quantum critical temperature $T_{c1} \propto \hbar^2$. Above T_{c1} there emerges a quantum crossover region where the switching rate displays a steep and characteristic temperature dependence, followed by a qualitatively different temperature dependence for higher T. In contrast to the crossover between tunneling and thermal activation in equilibrium systems, here the crossover occurs between different regimes of switching activated by quantum fluctuations. The results go beyond the standard real-time instanton technique of the large-deviation theory.

DOI: 10.1103/PhysRevA.87.062117 PACS number(s): 03.65.Yz, 05.40.−a, 85.25.Cp, 85.85.+j

I. INTRODUCTION

A modulated nonlinear oscillator models many well-controlled systems currently studied in cavity and circuit quantum electrodynamics, nanomechanics, and other areas [1]. This makes the oscillator advantageous for exploring quantum physics far from thermal equilibrium. Of fairly general interest in this respect are large rare quantum fluctuations that lead to switching between coexisting stable vibrational states (SVSs) and the occurrence of switching mechanisms that have no analog in equilibrium systems. The switching is important also for applications in quantum information [2–9]. For a resonantly modulated oscillator, a major quantum mechanism of switching is quantum activation [10,11]: transitions over an effective barrier due to diffusion over oscillator eigenstates. It recalls thermal activation [12], except that the diffusion is due to quantum fluctuations that come along with the oscillator relaxation, with $\hbar$ playing the role of temperature in thermal activation. Quantum activation was first seen in the experiment reported in [2].

A well-known effect in switching of thermal equilibrium systems is the crossover from quantum tunneling to overbarrier transitions, which occurs for $k_BT = \hbar\omega_{\rm ch}$, where $\omega_{\rm ch}$ is a characteristic system frequency [13,14]. In contrast, and surprisingly, the switching rates of a modulated oscillator $W_{\rm sw}$ calculated in the WKB-type approximation for $T = 0$ [15] and $T > 0$ can differ exponentially strongly even where in the $T > 0$ region the appropriately scaled ratio $T/\hbar \to 0$ [10,11]. Both for $T = 0$ and $T > 0$ switching occurs via transitions over an effective barrier rather than tunneling, but for $T > 0$ the system lacks detailed balance.

In this paper we study the low-temperature behavior of the oscillator switching rate $W_{\rm sw}$ and the crossover between the switching with and without detailed balance. The crossover has pronounced characteristic features accessible to direct experimental observation with the currently available systems. The conventional WKB-type approximation of the theory of rare events, the real-time instanton technique [16,17], does not apply in the crossover region, since the tail of the probability distribution has different decay lengths on the opposite sides of this region (both of them temperature independent). Our approach overcomes this problem. It bears also on rare events in chemical kinetics and population dynamics, where similar crossovers may occur [18].

Quantum states of a periodically modulated oscillator are the quasienergy (Floquet) states [19]. Coupling of the oscillator to a thermal reservoir leads to transitions between them and thus to oscillator relaxation toward SVSs. In a simple picture relaxation comes from emission of excitations of the bath, for example, photons with energy $\approx\hbar\omega_0$, where ω_0 is the oscillator eigenfrequency. The relaxation is accompanied by noise, because photons are emitted at random. The noise leads to oscillator fluctuations and diffusion away from SVSs. For $T > 0$, along with the noise from photon emission, there is noise from photon absorption. Its intensity is proportional to the oscillator Planck number $\bar{n} = [\exp(\hbar\omega_0/k_BT) - 1]^{-1}$.

An insight into the oscillator dynamics can be gained from Fig. 1. It shows the scaled Hamiltonian $g(Q,P)$ of a nonlinear oscillator modulated at frequency $\omega_F \approx \omega_0$. It is obtained in the rotating-wave approximation (RWA) from the full Hamiltonian $H_0 = \frac{1}{2}p^2 + \frac{1}{2}\omega_0^2q^2 + \frac{1}{4}\gamma q^4 - Aq\cos(\omega_F t)$ by changing to the rotating frame using the transformation $U(t) = \exp(-i\omega_F a^\dagger a t)$. Here (q,p) and (Q,P) are the oscillator coordinates and momenta in the laboratory and rotating frame, respectively, and $a^\dagger$ and a are the raising and lowering operators (cf. [3,4,10]),

$$g(Q,P) = \tfrac{1}{4}(Q^2 + P^2 - 1)^2 - \beta^{1/2}Q, \quad [Q,P] = i\lambda; \qquad (1)$$

$\beta = 3|\gamma|A^2/32\omega_F^3|\omega_F - \omega_0|^3$ is the scaled field intensity and $\lambda = 3\hbar\gamma/8\omega_F^2(\omega_F - \omega_0)$ is the scaled Planck constant.

The extrema of $g(Q,P)$ correspond to the SVSs in the weak-damping limit. Quasienergy states localized about an extremum are analogous to intrawell quantum states of a particle in a static potential. We count them off from the corresponding extremum.

*Present address: Institute for Theoretical Physics II, University of Erlangen-Nuremberg, 91058 Erlangen, Germany.

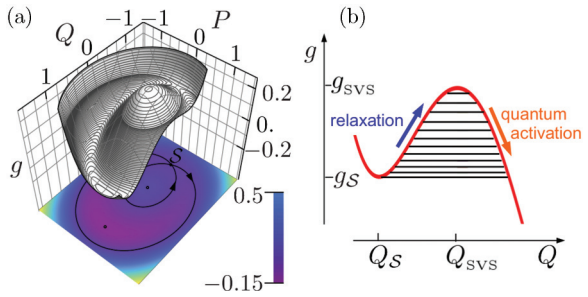

FIG. 1. (Color online) (a) The scaled Hamiltonian $g(Q,P)$ of the resonantly driven nonlinear oscillator; Q and P are the dimensionless coordinate and momentum in the rotating frame. In the presence of weak dissipation, the local maximum and minimum of g correspond to the small- and large-amplitude stable vibrational states. The scaled field intensity is $\beta = 0.02$. (b) The cross section $g(Q,0)$; the solid lines show the quasienergy states localized about the local maximum $g_{\rm SVS}$ for $\lambda = 0.015$. Their scaled quasienergies g_n lie between $g_{\rm SVS}$ and the value of $g(Q,P)$ at the saddle point, g_S.

II. BALANCE EQUATION AND THE EIKONAL APPROXIMATION

For weak damping, the state populations ρ_n are given by a balance equation. In slow time $\tau = |\omega_F - \omega_0|t$

$$\dot\rho_n \equiv d\rho_n/d\tau = \sum_m (W_{mn}\rho_m - W_{nm}\rho_n). \qquad (2)$$

We are interested in solving this equation in the WKB limit $\lambda \ll 1$ where the number of localized states $M \sim 1/\lambda \propto 1/\hbar$ is large. In this limit Eq. (2) is similar to the balance equations studied in chemical kinetics and population dynamics, with M playing the role of the number of molecules or the total population [17]. On times large compared to the oscillator relaxation time but small compared to the reciprocal switching rate, the distribution ρ_n becomes quasistationary. It can be sought in the eikonal form

$$\rho_n = \exp(-R_n/\lambda), \quad R_n \equiv R(g_n); \quad \lambda \ll 1. \qquad (3)$$

Here g_n is the eigenvalue of g in quantum state n, i.e., the scaled quasienergy of state n. The dimensionless rate of switching from the initially occupied SVS $W_{\rm sw}$ is determined by the population of states with quasienergies g_n close to the saddle-point quasienergy g_s in Fig. 1 [12],

$$W_{\rm sw} \sim \kappa \exp(-R_A/\lambda), \quad R_A = R(g_s), \qquad (4)$$

where κ is the oscillator decay rate scaled by $|\omega_F - \omega_0|$.

The central approximation of the real-time instanton approach is that in Eq. (3) R_n smoothly varies with n, so that $|R_{n+m} - R_n| \approx m\partial_n R_n$ for $|m| \ll 1/\lambda$, with $|\partial_n R_n| \propto \lambda \ll 1$. This approximation can break down in a nontrivial way, and in what follows we show how to find ρ_n where this happens.

The dimensionless transition rates W_{mn} for $|m-n| \ll 1/\lambda$ for a modulated oscillator were calculated earlier [10] and are given for completeness in Appendix A. Oscillator relaxation corresponds to transitions toward the SVS and is described by rates W_{mn} with $m > n$. Transitions with $m < n$ lead to diffusion away from the SVS.

The rates $W_{mn} = W_{mn}^{(\rm e)} + W_{mn}^{(\rm abs)}$ have two terms, which come from emission and absorption of bath excitations, respectively; $W_{mn}^{(\rm abs)} \propto \bar n$. Both terms exponentially decay with increasing $|n-m|$. However, the decay of $W_{mn}^{(\rm abs)}$ with increasing $n - m > 0$ is slower, as can be seen from Eqs. (A2) and (A3). It is this difference that is at the root of the discussed behavior.

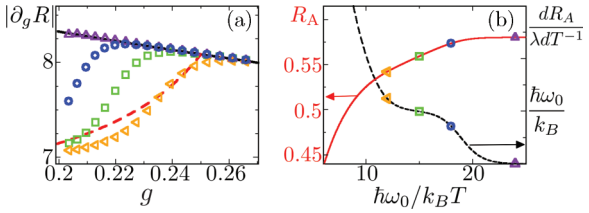

FIG. 2. (Color online) (a) The steepness of the distribution eikonal $|\partial_g R|$ calculated numerically as $(\partial_g R)_{g_n} = \nu(g_n)^{-1}\ln(\rho_n/\rho_{n-1})$. The results refer to the temperatures marked on the right panel by the corresponding symbols; $\beta = 0.0448$ and $\lambda = 0.0053$ (for such parameters, the number of states localized about the small-amplitude SVS is $M = 20$). The solid and dashed lines show $|\partial_g R|$ for $\bar n = 0$ and $\bar n \to 0$ but $T > T_{c2}$, respectively. (b) The activation exponent R_A calculated numerically from Eq. (2) (solid curve) and the derivative $dR_A/\lambda dT^{-1} \approx -d\ln W_{\rm st}/dT^{-1}$ (dashed curve). The units on the right axis are kelvins.

The ratio of the emission-induced rates is

$$W_{n\,n+k}^{(\rm e)}/W_{n+k\,n}^{(\rm e)} = \exp(-k/\xi_n) \quad (\xi_n > 0) \qquad (5)$$

for $|k| \ll 1/\lambda$. The decay length $\xi_n \equiv \xi(g_n)$ smoothly varies with n. It is expressed in terms of the parameters of the classical orbits $Q(\tau;g)$ of a system with Hamiltonian $g(Q,P)$: $\xi(g) = \{2\nu(g){\rm Im}[\tau_p^{(2)}(g) - 2\tau_*(g)]\}^{-1}$. Here, $\nu(g)$ is the vibration frequency of the system, $\tau_*(g)$ is the time it takes for Q to go to infinity, and $\tau_p^{(2)}(g)$ is the complex period [the orbits $Q(\tau;g)$ are double periodic; the real period is $2\pi/\nu(g)$].

From Eqs. (2) and (5), for $T = 0$ we obtain for the quasistationary distribution $\rho_n^{(0)}$ and the eikonal $R_n^{(0)}$

$$\rho_{n+k}^{(0)}/\rho_n^{(0)} = \exp(-k/\xi_n), \quad \partial_n R_n^{(0)} = \lambda/\xi_n. \qquad (6)$$

The function $\partial_{g_n} R^{(0)}(g_n) \equiv \partial_n R_n^{(0)}/\partial_n g_n$ is shown in Fig. 2. One can associate $\partial_g R^{(0)}/\lambda$ with the effective reciprocal temperature of the quasienergy distribution; this temperature itself depends on the quasienergy, $\rho_n^{(0)} \propto \exp[-\int^{g_n} dg\,\partial_g R^{(0)}(g)/\lambda]$.

Absorption-induced transitions between the oscillator states perturb the $T = 0$ distribution. Because of the comparatively slow decay of $W_{mn}^{(\rm abs)}$ with $n - m$ for $n > m$, the major perturbation comes from the absorption-induced influx from more populated states, which are closer to the extremum of $g(Q,P)$. For a state n, from Eq. (2) this influx scaled by the $T = 0$ rate of leaving the state $W_n^{(\rm e)}\rho_n$ ($W_n^{(\rm e)} = \sum_m W_{nm}^{(\rm e)}$) is

$$\varkappa_n = \sum_{m<n} w_{mn}/W_n^{(\rm e)}, \quad w_{mn} = W_{mn}^{(\rm abs)}\rho_m/\rho_n. \qquad (7)$$

To the leading order in $\bar n$, in Eq. (7) $\varkappa_n \to \varkappa_n^{(0)}$, $w_{mn} \to w_{mn}^{(0)}$, where the zeroth-order scaled influx $w_{mn}^{(0)} = W_{mn}^{(\rm abs)}\rho_m^{(0)}/\rho_n^{(0)}$. If the rates $W_{n-k\,n}^{(\rm abs)}$ decay with increasing k more slowly than $\exp(-k/\xi_n)$, the parameters $w_{n-k\,n}^{(0)}$ increase with increasing k. This leads to *nonlocality*: the relative influx (7) is dominated by remote states m with $n - m \gg 1$. In contrast, because of the lack of detailed balance, the flux *from* a state n is still dominated by emission-induced processes,

$\sum_m W_{nm} \approx W_n^{(e)}$. Therefore in the limit $\lambda \to 0$, where the number of localized states $M \to \infty$, the perturbation theory diverges.

III. BEYOND THE CONVENTIONAL LARGE-DEVIATION THEORY

In what follows we solve the balance equation in the parameter range where the zeroth-order scaled influx $w_{mn}^{(0)}$ increases with $n-m$. Our method is fairly general and it shows how one can go beyond the conventional large-deviation theory when the perturbation is singular. For concreteness, we analyze the distribution about the small-amplitude SVS, i.e., about the local maximum of $g(Q,P)$ in Fig. 1, which is of primary interest for the experiment; cf. [2,5]. Since of importance are $n-m \sim 1/\lambda \gg 1$, it is necessary first to find the transition rates W_{mn} for large $n-m$, where they are exponentially small. This can be done in the WKB approximation by extending the conformal mapping technique [20]. The calculation gives both the exponent and the prefactor in W_{mn}; see Appendix B.

The explicit expressions for ξ_n and W_{nm} show that

$$w_{mn}^{(0)} \propto \bar{n}\lambda^{-3} \exp\left[\lambda^{-1}\int_{g_n}^{g_m} dg f(g)\right]$$

[for states localized about the local maximum of $g(Q,P)$, $g_n < g_m$ for $n > m$]. The function $f(g) = 2\mathrm{Im}[\tau_p^{(2)}(g) - 3\tau_*(g)]$ monotonically decreases with increasing g and goes through 0 for $g = g_e$; in our model $g_e = 1/4$ independent of the scaled field intensity β in Eq. (1). Therefore $w_{mn}^{(0)}$ displays a sharp maximum as a function of m for g_m closest to g_e. Calculating $\sum_m w_{mn}^{(0)}$ by the steepest-descent method, we obtain from Eq. (7)

$$\varkappa_n^{(0)} = C_n \bar{n}\lambda^{-5/2} \exp\left[\lambda^{-1}\int_{g_n}^{g_e} f(g')dg'\right]; \tag{8}$$

here, $C_n \propto (g_e - g_n)^2$ is independent of λ and T [see Eq. (C2)].

The condition $\varkappa_n^{(0)} \sim 1$ (more precisely, $|\varkappa_n^{(0)} - 1|$ is minimal) defines the characteristic level number $n_\varkappa$ and quasienergy $g_{n_\varkappa} \equiv g_\varkappa(T)$ for given T as well as the characteristic temperature $T_\varkappa(g_n)$ for given g_n where the $T = 0$ expression for the distribution (6) ceases to apply.

To allow for the thermally induced modification of the probability distribution we seek it in the form (3) with $R_n = R_n^{(0)} + \Delta_n$. This is *not* a perturbative solution; we do *not* assume that $|\Delta_n|$ is small or smoothly varying with n. As we will see, $|\Delta_n|$ remains small in a part of the distribution and is large but smooth as a function of n in another part. In these parts R_n is thus smooth, too. It is of critical importance that the transition between the corresponding regions of n occurs in a narrow range, and in this range R_n steeply changes with n, in contrast to the conventional assumption of the large-deviation theory.

For small $\bar{n}$ we need to consider the absorption-induced transitions to a given state n only from states m with $m < n$. Then the balance equation in the quasistationary regime reads

$$\sum_m \left(W_{nm}^{(e)}/W_n^{(e)}\right) e^{(\Delta_n - \Delta_m)/\lambda} - 1 = -\varkappa_n. \tag{9}$$

From Eq. (7), $\varkappa_n \equiv \sum_{m<n} w_{mn}^{(0)} \exp[(\Delta_n - \Delta_m)/\lambda]/W_n^{(e)}$.

We start with the distribution for states n comparatively close to the extremum of g, $n_\varkappa - n \gg 1$. For such n we expect the correction to ρ_n to be small. Respectively, in Eq. (9) we replace $\varkappa_n$ with $\varkappa_n^{(0)}$ and expand the left-hand side to first order in Δ_n, Δ_m, which gives

$$\Delta_n = -\lambda\varkappa_n^{(0)}/a_n. \tag{10}$$

The parameter $a_n > 0$ is given in Eq. (C3); $a_n \sim 1$ and is independent of λ. From Eqs. (8) and (10), $|\Delta_n|$ is exponentially small for large $n_\varkappa - n$ but increases with n exponentially fast.

For states with $n > n_\varkappa$, the absorption-induced influx into a state is no longer small and must be balanced by emission-induced transitions from the state, which means $\varkappa_n \sim 1$. It is convenient to split the sum over m in $\varkappa_n$ in Eq. (7) into a sum from $n-1$ to $n_\varkappa - \delta n$ and a sum over $m < n_\varkappa - \delta n$, where $1 \ll \delta n \ll 1/\lambda$. We denote these sums as $\varkappa_n'$ and $\varkappa_n''$, respectively. In calculating $\varkappa_n''$, in the sum over m one can approximate ρ_m by $\rho_m^{(0)}$, since the correction Δ_m, Eq. (10), is exponentially small for $n_\varkappa - m \gg 1$. Taking into account the exponential dependence of $w_{mn}^{(0)}$ on m and n, one can see that the leading contribution to $\varkappa_n''$ comes from transitions from remote states with $g_m \approx g_e$,

$$\begin{aligned} \varkappa_n' &= \sum_{m=n_\varkappa-\delta n}^{n-1} \left(w_{mn}^{(0)}/W_n^{(e)}\right) e^{(\Delta_n - \Delta_m)/\lambda}, \\ \varkappa_n'' &\approx \varkappa_n^{(0)}\rho_n^{(0)}/\rho_n. \end{aligned} \tag{11}$$

We first consider the temperature range where $\bar{n} \ll \lambda^3$, which includes the limit $T \to 0$. Here, as seen from Eq. (12) below, we can disregard the term $\varkappa_n'$ in $\varkappa_n$. Then from Eqs. (8), (9), and (11) and from the condition $\varkappa_{n_\varkappa}^{(0)} \sim 1$ we obtain

$$\Delta_n \approx -\int_{g_n}^{g_\varkappa} dg f(g), \quad n - n_\varkappa \gg 1. \tag{12}$$

In contrast to the exponentially steep n dependence of Δ_n for $n < n_\varkappa$ in Eq. (10), Δ_n of the form (12) smoothly depends on n. Corrections to Eq. (12) come from the approximations made in Eqs. (8) and (11) and the dependence on n of the left-hand side of Eq. (9). They are $\sim\lambda$. From the expression for $w_{mn}^{(0)}$ and Eq. (11), for Δ_n of the form (12) $\varkappa_n' \lesssim \bar{n}/\lambda^3 \ll \varkappa_n''$.

For $\lambda^{3/2} \gg \bar{n} \gg \lambda^3$, on the other hand, transitions to states with $n - n_\varkappa \gg \bar{n}^{1/3}$ are balanced locally and $\varkappa_n' \gg \varkappa_n''$. The analysis of this case is similar, and the leading term in Δ_n is still given by Eq. (12), but Δ_n has an important correction $\sim \bar{n}^{1/3}$; see Appendix C.

The boundary layer between the solutions (10) and (12) is centered at $n_\varkappa$ and has width $|n - n_\varkappa| \sim 1$. Inside the layer $|\Delta_n| \sim \lambda$ is given by the full equation (9).

Equations (6) and (12) give the eikonal of the probability distribution in the explicit form, with $R_n \approx R_n^{(0)}$ for $n_\varkappa - n \gg 1$ and $R_n \equiv R_n^{(T)} \approx R_n^{(0)} + \Delta_n$, where Δ_n is of the form (12) for $n - n_\varkappa \gg 1$. For $|n - n_\varkappa| \gg 1$ the derivative $\partial_n R_n$ is smooth. In the region $|n - n_\varkappa| \sim 1$ it displays a kink. It sharply drops with increasing n from λ/ξ_n for $n_\varkappa - n \gg 1$ to $\lambda[\xi_n^{-1} - \nu_n f(g_n)]$ for $n - n_\varkappa \gg 1$. The kink is seen in the numerical data in Fig. 2(a).

IV. CONCLUSIONS

The kink of the exponent of the probability distribution, i.e., of $\ln(\rho_n/\rho_{n-1})$, is a singular modification of the distribution compared to the prediction of the conventional real-time instanton approach. Remarkably, it emerges where the perturbation formally remains small compared to the WKB parameter. In the present case, the corresponding condition is $\bar{n} \ll \lambda \propto \hbar$. One might hypothesize that this is a generic feature of the breakdown of the real-time instanton approach.

In the underdamped modulated oscillator, with increasing T the kink emerges at the critical temperature $T_{c1} = T_{\varkappa}(g_S)$. This is because $\varkappa_n^{(0)}$ as given by Eq. (8) monotonically increases with n, and therefore the condition $\varkappa_n^{(0)} \approx 1$ is first met with increasing T at the saddle point, $g_n \approx g_S$, where n is maximal. From Eq. (8)

$$T_{c1} = \hbar\omega_0\lambda \Big/ \int_{g_S}^{g_e} dg f(g) \propto \hbar^2.$$

For $T < T_{c1}$ the distribution ρ_n and the switching rate $W_{\rm sw}$ are well described by the $T = 0$ expressions.

For $T > T_{c1}$, the kink of $\partial_n R_n$ moves with the increasing T from $g_n \approx g_S$ to $g_n \approx g_e$. From Eq. (8), it approaches g_e and disappears for $\bar{n} \sim \lambda^{3/2}$ or $T \sim T_{c2} = \hbar\omega_0/k_B|\ln\lambda|$, still deep in the quantum domain, $T_{c2} \propto \hbar/|\ln\hbar|$. For $T_{c1} < T < T_{c2}$ the effective switching activation energy $R_A \approx \lambda|\ln W_{\rm sw}|$ is

$$R_A \approx \int_{g_{\rm SVS}}^{g_{\varkappa}} dg\,\partial_g R^{(0)}(g) + \int_{g_{\varkappa}}^{g_S} dg\,\partial_g R^{(T)}(g) \qquad (13)$$

[$g_{\rm SVS}$ is the quasienergy of the occupied SVS; from Eq. (12), $\partial_g R^{(T)} = \partial_g R^{(0)} + f(g)$]. It depends on T through $g_{\varkappa}$ and, for $\bar{n} \gg \lambda^3$, through $R^{(T)}$.

From Eq. (8),

$$d\ln W_{\rm sw}/dT^{-1} \approx -(\hbar\omega_0/k_B) \quad \text{for} \quad \bar{n} \ll \lambda^3,$$

i.e., the slope of the logarithm of the switching rate displays a plateau with height independent of the modulation. This unexpected behavior emerges because remote quasienergy states are populated nonlocally, through the influx directly from the states close to the SVS, with transition rates $\propto\bar{n}$. It is confirmed by numerical simulations; see Fig. 2.

The plateau of $d\ln W_{\rm sw}/dT^{-1}$ appears even in the ultraquantum regime, where only a few states are localized about the extremum of $g(Q,P)$. Here, too, the population of excited localized states is determined by absorption-induced transitions from the vicinity of the SVS with rates $\propto\bar{n}$. This regime may be easier to access in the experiment, as the switching rates are larger. We take as an example a Josephson resonator with eigenfrequency $\omega_0 = 2\pi \times 6.5$ GHz, one-photon resonance shift $V = -3\hbar\gamma/4\omega_0^2 = 2\pi \times 8$ MHz, relaxation rate $\Gamma = 2\pi \times 2$ MHz, and dimensionless parameters $\lambda = 0.102$ and $\beta = 1/300$ [Rabi frequency $A(2\hbar\omega_F)^{-1/2} \approx 2\pi \times 10$ MHz, detuning $\omega_F - \omega_0 = -2\pi \times 39$ MHz, and the number of localized states $M = 4$]. Then $W_{\rm sw} \approx 10^{-2}$ Hz for $T < T_{c1} \approx 20$ mK whereas $W_{\rm sw} \approx 4$ Hz at the end of the plateau for $T \approx 40$ mK. With parameters leading to larger λ one can access larger switching rates.

In conclusion, we have studied the probability distribution and switching of a resonantly modulated nonlinear quantum oscillator. We find a region of quantum crossover of the switching rate, which lies between the critical temperatures $T_{c1} \propto \hbar^2$ and $T_{c2} \propto \hbar/|\ln\hbar|$. In this region the slope of the *logarithm* of the oscillator distribution over quasienergy states, which is the analog of the effective reciprocal temperature for this distribution, displays a kink. The slope changes from the $T = 0$ value, where the dissipation-induced interstate transitions are balanced within a few nearest states, to the value where long-range transitions are important. As a consequence, in the deeply quantum regime the temperature dependence of the oscillator switching rate mimics the activation law with the activation energy $\hbar\omega_0$ independent of the modulation strength. The results bear on the current experiments on nonlinear cavity modes and modulated Josephson junctions.

ACKNOWLEDGMENTS

We are grateful to G. Schön for an insightful discussion. V.P. and M.I.D. acknowledge support from the NSF, Grant No. EMT/QIS 082985, and the ARO, Grant No. W911NF-12-1-0235.

APPENDIX A: MATRIX ELEMENTS BETWEEN CLOSE QUASIENERGY STATES

For completeness, we first give the rates of transitions between close eigenstates of the oscillator Hamiltonian in the rotating frame $g(Q, -i\lambda\partial_Q)$, which is defined in Eq. (1) (see [10,11]). The function $g(Q,P)$ has the shape of a tilted Mexican hat; see Fig. 1. Our analysis refers to the states localized about the local maximum of $g(Q,P)$, and we count the states off from this maximum.

Interstate transitions result from the oscillator coupling to a thermal reservoir. For a weak coupling, the dynamics of the resonantly modulated oscillator can often be described in slow time $\tau = |\omega_F - \omega_0|t$ by a Markov master equation for the oscillator density matrix ρ. To the lowest order in the coupling, the coupling-induced term in this equation has a familiar form [21],

$$(d\rho/d\tau)_{\rm cpl} = -\kappa(\bar{n}+1)(a^\dagger a\rho - 2a\rho a^\dagger + \rho a^\dagger a) - \kappa\bar{n}(aa^\dagger\rho - 2a^\dagger\rho a + \rho aa^\dagger). \qquad (A1)$$

We assumed here that the coupling is linear in the oscillator raising and lowering operators $a^\dagger$ and a. The coupling-induced renormalization of the oscillator parameters has been incorporated into their values; κ is the scaled oscillator decay rate. It has not been assumed that the coupling leads to Ohmic dissipation. The approximation involved relies on the smallness of corrections $\sim(\partial\kappa/\partial\omega_0)\Delta\omega, \kappa\Delta\omega/\omega_0$ and similar corrections for the polaronic frequency shift. Here, $\Delta\omega$ includes the frequency detuning of the driving field $\omega_F - \omega_0$ and the nonlinear shift of the eigenfrequency with vibration amplitude, for typical amplitudes (for thermally excited vibrations, this shift depends on temperature, but this case is not of interest for this paper). An extra confirmation of the applicability of Eq. (A1) is that, in the absence of modulation, its results coincide [22] with the results obtained with the double-time Green's function technique [23], which apply for arbitrary temperature.

From Eq. (A1), the scaled rates of transitions between the eigenstates ψ_m and ψ_n due to emission and absorption of

excitations of the thermal reservoir are, respectively,

$$W^{(e)}_{mn} = 2\kappa(\bar{n}+1)|a_{nm}|^2, \quad W^{(abs)}_{mn} = \frac{\bar{n}}{\bar{n}+1} W^{(e)}_{nm}. \tag{A2}$$

Here, $a_{mn} \equiv \langle \psi_m | a | \psi_n \rangle = (2\lambda)^{-1/2}(Q + iP)_{mn}$.

If the dimensionless Planck constant λ for motion in the rotating frame is small, $\lambda \ll 1$, one can find a_{mn} using the WKB approximation for $\psi_n(Q)$. A significant simplification comes from the fact that the classical trajectories $Q(\tau; g)$ of the system with Hamiltonian $g(Q,P)$ are described by the Jacobi elliptic functions; $Q(\tau; g)$ is double periodic on the complex-τ plane, with real period $\tau_p^{(1)}(g)$ and complex period $\tau_p^{(2)}(g)$ [10]. For $|m-n| \ll \lambda^{-1}$ the matrix element a_{mn} is given by the Fourier $m-n$ component of the function $a(\tau; g) = (2\lambda)^{-1/2}[Q(\tau; g) + iP(\tau; g)]$ [24]. In turn, this gives

$$W^{(e)}_{n\,n+k} = \frac{\kappa(\bar{n}+1)k^2 v_n^4}{\beta\lambda} \frac{\exp\left[k v_n \operatorname{Im}\left(2\tau_* - \tau_p^{(2)}\right)\right]}{\left|\sinh\left[ik v_n \tau_p^{(2)}/2\right]\right|^2}. \tag{A3}$$

Here, $\tau_* \equiv \tau_*(g_n)$ and $\tau_p^{(2)} \equiv \tau_p^{(2)}(g_n)$ ($\operatorname{Im}\tau_*, \operatorname{Im}\tau_p^{(2)} > 0$); $\tau_*(g_n)$ is the pole of $Q(\tau; g_n)$ closest to the real axis; $\nu_n = 2\pi/\tau_p^{(1)}(g_n)$ is the dimensionless frequency of vibrations in the rotating frame with quasienergy g_n. To the leading order in λ, we have $W^{(e)}_{n\,n+k} = W^{(e)}_{n-k\,n}$. Equation (A3) has to be modified for states very close to the extrema of $g(Q,0)$; this modification is straightforward.

APPENDIX B: MATRIX ELEMENTS BETWEEN REMOTE QUASIENERGY STATES

In this Appendix we calculate in the WKB approximation the exponent and the prefactor of the matrix element a_{mn} for remote eigenstates ψ_m and ψ_n. The approach we use is similar, but not identical, to that developed [20] in the problem of a parametrically modulated oscillator. First, in the spirit of Ref. [24], we write

$$a_{mn} = \operatorname{Re}\int_{-\infty}^{\infty} dQ\, a_+(Q), \quad n > m, \tag{B1}$$

$$a_+(Q) = \psi_m(Q)(Q + \lambda\partial_Q)\psi_n^+(Q)/\sqrt{2\lambda}.$$

The function $\psi_n^+(Q)$ is an eigenfunction of operator $g(Q, P = -i\lambda\partial_Q)$ such that $\operatorname{Re}[\psi_n^+(Q)] = \psi_n(Q)$ and that slightly above the real Q axis in the WKB approximation

$$\psi_n^+(Q) \approx \left(\frac{-2\nu_n}{\pi\,\partial_P g_n}\right)^{1/2} \exp[i\lambda^{-1}S_n(Q) + i\pi/4]. \tag{B2}$$

Here, $\partial_P g_n$ is $\partial_P g$ calculated for the momentum $P = P(Q, g_n)$; $S_n(Q)$ is the mechanical action counted off from the right turning point $Q_R(g_n)$ of the classical orbit that lies on the inner dome of the function $g(Q,P)$ shown in Fig. 1, with $g(Q,P) = g_n$. For the inner-dome orbits the momentum is

$$P(Q,g) = \sqrt{1 - Q^2 - 2\sqrt{g + \beta^{1/2}Q}}, \tag{B3}$$

and $S_n(Q) = \int_{Q_R(g_n)}^{Q} P(Q', g_n)\,dQ'$.

The WKB approximation does not apply to the function $a_+(Q)$ close to the zeros and the branching points of $P(Q, g_n)$ and $P(Q, g_m)$. We go around these points by lifting the integration contour above the real Q axis.

On the real-Q axis the WKB wave function $\psi_m(Q)$ in Eq. (B1) is $\psi_m(Q) \propto \cos[\lambda^{-1}S_m(Q) + \pi/4]$ for Q in the interval between the left and right turning points, $Q_L(g_m)$ and $Q_R(g_m)$. Above this interval on the complex-Q plane one of the terms in the cosine becomes exponentially small and should be disregarded in the WKB approximation [24], so that

$$\psi_m(Q) \approx \left(\frac{-\nu_m}{2\pi\,\partial_P g_m}\right)^{1/2} \exp[-i\lambda^{-1}S_m(Q) - i\pi/4]. \tag{B4}$$

We will illustrate the calculation by considering the case $g_m < \sqrt{\beta}$. For such g, the orbits on the external part of $g(Q,P)$ have the shape of a horseshoe. The function $P(Q, g_m)$ as given by Eq. (B3) has a branching point $Q_B = -g/\sqrt{\beta}$, which corresponds to the two utmost negative-Q points of the horseshoe. It also has three zeros: $Q_R(g_m)$, $Q_L(g_m)$, and $Q_{\text{ext}}(g_m)$ on the real-Q axis, with $Q_B < Q_{\text{ext}} < Q_L < Q_R$.

To calculate the integral in Eq. (B1) we change in the range $Q > Q_{\text{ext}}$ to integration over a contour $\mathcal{C}$ shown in Fig. 3(a). On this contour, from Eqs. (B1), (B2), and (B4),

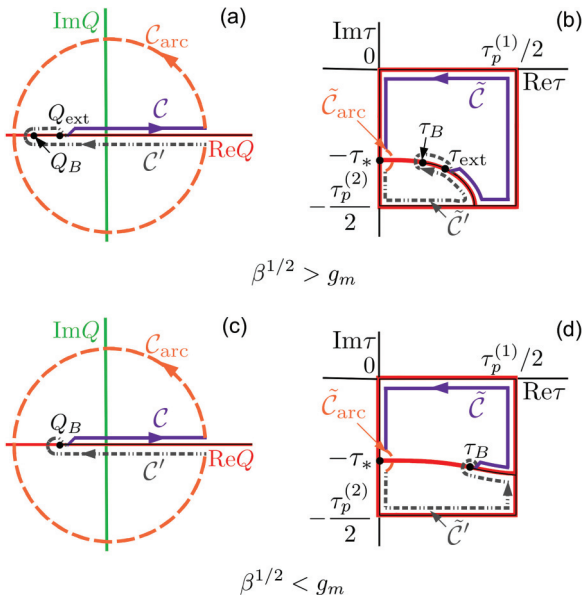

FIG. 3. (Color online) (a) The contour of integration $\mathcal{C}$ for calculating the matrix element (B6) in the WKB approximation and the auxiliary integration contours $\mathcal{C}'$ and $\mathcal{C}_{\text{arc}}$ for $g_m < \sqrt{\beta}$; $Q_B \equiv Q_B(g_m)$ and $Q_{\text{ext}} \equiv Q_{\text{ext}}(g_m)$ are the branching point and turning point of $P(Q, g_m)$; see Eq. (B3). (b) Mapping of the Q plane (with a branch cut from Q_{ext} to ∞, the black thin line in (a)) on the interior of a rectangle on the τ plane for $g_m < \sqrt{\beta}$ by the function $Q(\tau; g)$ that describes the classical Hamiltonian trajectory with given g, $g_n < g < g_m$; $\tau_p^{(1)}$, $\tau_p^{(2)}$, and τ_* are the real and imaginary periods and the pole of $Q(\tau; g)$, respectively. The solid ($\tilde{\mathcal{C}}$), dashed ($\tilde{\mathcal{C}}_{\text{arc}}$), and dash-dotted ($\tilde{\mathcal{C}}'$) lines are the maps of the corresponding contours in (a). The solid arc in the lower left corner is the map of the real axis of Q from $-\infty$ to $Q_B(g)$; τ_B and τ_{ext} are the times for reaching $Q_B(g_m)$ and $Q_{\text{ext}}(g_m)$. (c) Integration contours for $g_m > \sqrt{\beta}$. (d) Conformal mapping for $g > \sqrt{\beta}$. The curved red line dividing the rectangle into two parts is the map of the real axis of Q from $-\infty$ to $Q_B(g)$.

$a_+(Q) \approx a_+^{\rm WKB}(Q)$ with

$$a_+^{\rm WKB}(Q) \equiv \pi^{-1}(\nu_n\nu_m/2\lambda\partial_P g_n \partial_P g_m)^{1/2} \times [Q + iP(Q,g_n)]\exp\{i[S_n(Q) - S_m(Q)]/\lambda\}. \quad \text{(B5)}$$

It is straightforward to show using the full expression for $\psi_m(Q)$ that the real part of the exponent in the expression for $a_+(Q)$ monotonically increases on the interval $(-\infty, Q_{\rm ext}]$. Therefore, to logarithmic accuracy the upper bound of the contribution of the integral from $-\infty$ to $Q_{\rm ext}$ of $a_+(Q)$ in Eq. (B1) is $\sim a_+(Q_{\rm ext}) \sim a_+^{\rm WKB}(Q_{\rm ext})$. Below we show that a_{mn} is exponentially larger than $a_+^{\rm WKB}(Q_{\rm ext})$. Then

$$a_{mn} \approx {\rm Re}\int_{\mathcal{C}} dQ a_+^{\rm WKB}(Q). \quad \text{(B6)}$$

To evaluate the integral (B6), we analytically continue $a_+^{\rm WKB}$ to the Q plane with a branch cut on the semi-infinite interval $[Q_B(g_m),\infty)$. We then can change from integration along $\mathcal{C}$ to integration along the circle $\mathcal{C}_{\rm arc}$ and contour $\mathcal{C}'$ shown in Fig. 3(a).

The function $Q(\tau; g)$, which describes the classical trajectory for the Hamiltonian $g(Q,P)$, provides conformal mapping of the Q plane (with a branch cut) onto a g-dependent region on the plane of complex time τ. We define $\tau(Q,g)$ as the duration of classical motion from the turning point $Q_R(g)$ to Q. Then the region of the τ plane that corresponds to the Q plane (with a branch cut) is the interior of a rectangle shown in Fig. 3(b).

Since $\tau(Q,g) = \partial S/\partial g$, the exponent in Eq. (B5) is

$$\frac{i}{\lambda}[S_n(Q) - S_m(Q)] = -\frac{i}{\lambda}\int_{g_n}^{g_m} dg\tau(Q,g). \quad \text{(B7)}$$

As seen in Fig. 3(b), for any g between g_n and g_m, for any $Q_{\rm arc}$ on contour $\mathcal{C}_{\rm arc}$ and any Q' on contour $\mathcal{C}'$, $|{\rm Im}\,\tau(Q_{\rm arc},g)| < |{\rm Im}\,\tau(Q',g)|$. Therefore, $a_+^{\rm WKB}(Q)$ is exponentially smaller on contour $\mathcal{C}'$ than on contour $\mathcal{C}_{\rm arc}$, and the integral along $\mathcal{C}'$ can be disregarded. Moreover, $a_+^{\rm WKB}(Q_{\rm ext}(g_m)) \ll a_{mn}$, as assumed in Eq. (B6).

The integral along $\mathcal{C}_{\rm arc}$ can be evaluated using the asymptotic expressions $P \approx -iQ$, $g_P \approx i2\beta^{1/4}Q^{3/2}$,

$$\frac{i}{\lambda}[S_n(Q) - S_m(Q)] \approx \frac{i}{\lambda}\int_{g_n}^{g_m} dg\tau_*(g) + \frac{g_m - g_n}{\lambda\beta^{1/4}Q^{1/2}}. \quad \text{(B8)}$$

With Eq. (B8), the integral (B6) is reduced to a simple residue, which gives

$$a_{mn} = \left(\frac{2\nu_n\nu_m}{\beta\lambda^3}\right)^{1/2}(g_m - g_n)\exp\left[i\lambda^{-1}\int_{g_n}^{g_m} dg\tau_*(g)\right]. \quad \text{(B9)}$$

For $g_m > \sqrt{\beta}$, the small-momentum branch $P(Q,g_m)$ (B3) has only two turning points. In the WKB approximation, $a_+(Q) \approx a_+^{\rm WKB}(Q)$ on contour $\mathcal{C}$ whose left end point is the branching point $Q_B(g_m)$; see Fig. 3(c). The conformal mapping $Q(\tau; g)$ has a different topology, which is shown in Fig. 3(d). Nonetheless, using the same arguments as before, we arrive at the same expression (B9) for the matrix elements a_{mn}.

In Fig. 4 we compare the explicit analytical expression for the matrix elements a_{mn}, which includes both the exponent and the prefactor, with the numerical calculations based on solving the Schrödinger equation $\hat{g}\psi_n = g_n\psi_n$. The results are in excellent agreement.

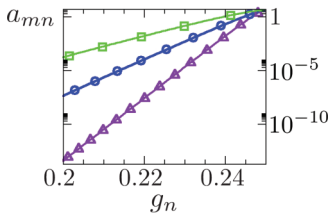

FIG. 4. (Color online) Comparison of Eq. (B9) for a_{mn} calculated as a continuous function of g_n (solid lines) with numerical calculations (symbols). The scaled intensity of the modulating field is $\beta = 0.0448$. The other parameter values are $\lambda = 0.0053$ and $m = 4$ (violet triangles), $\lambda = 0.09$ and $m = 2$ (blue circles), and $\lambda = 0.15$ and $m = 1$ (green squares). The parameter m has been chosen so that $g_m \approx g_e = 1/4$.

APPENDIX C: THERMALLY INDUCED MODIFICATION OF THE $T = 0$ DISTRIBUTION

The explicit expression for the transition matrix elements (B9) makes it possible to calculate the rate of absorption-induced transitions to a state n scaled by the rate of leaving this state $\varkappa_n^{(0)}$, which is given by Eq. (7) with ρ_m, ρ_n replaced by their $T = 0$ values $\rho_m^{(0)}, \rho_n^{(0)}$. The most probable transitions are those from states m closer to the SVS, $m < n$. From Eq. (B9), the term $w_{mn}^{(0)} = W_{mn}^{(\rm abs)}\rho_m^{(0)}/\rho_n^{(0)}$ in the expression for $\varkappa_n^{(0)}$ for $n - m \gg 1$ is of the form

$$w_{mn}^{(0)} \approx \bar{n}\kappa\lambda^{-3}C^{(w)}(g_m,g_n)\exp\left[\lambda^{-1}\int_{g_n}^{g_m} f(g)dg\right],$$
$$C^{(w)}(g_m,g_n) = (4\nu_m\nu_n/\beta)(g_m - g_n)^2, \quad \text{(C1)}$$

with $f(g) = 2{\rm Im}[\tau_p^{(2)}(g) - 3\tau_*(g)]$. As a function of m, $w_{mn}^{(0)}$ is maximal for g_m closest to the quasienergy value g_e given by the condition $f(g_e) = 0$.

Calculating the sum of $w_{mn}^{(0)}$ by the steepest-descent method, we obtain Eq. (8) for $\varkappa_n^{(0)}$ with

$$C_n = C^{(w)}(g_e,g_n)[2\kappa^2\pi/\partial_g f(g_e)]^{1/2}/\left(\lambda W_n^{(e)}\right). \quad \text{(C2)}$$

The overall rate $W_n^{(\rm e)}$ of emission-induced transitions from state n for $\bar{n} \ll 1$ can be found from Eq. (A3); using this equation we obtain $C_n \sim C^{(w)}(g_e,g_n)[2\pi/\partial_g f(g_e)]^{1/2}$.

The modification of the distribution $\rho_n^{(0)} = \exp(-R_n^{(0)}/\lambda)$ by absorption-induced transitions becomes substantial when $\bar{n}$ is still exponentially small in λ, $|\ln\bar{n}| \gtrsim \int_{g_S}^{g_e} f(g)dg/\lambda$. For small $\bar{n}$, the change Δ_n of the eikonal, $R_n = R_n^{(0)} + \Delta_n$, is described by Eq. (9). The solution of this equation for $n_\varkappa - n \gg 1$ is given by a simple perturbation theory and has the form of Eq. (10) of the main text with

$$a_n \approx \sum_m \left(W_{nm}^{(\rm e)}/W_n^{(\rm e)}\right)\{1 - \exp[(m-n)\nu(g_n)f(g_n)]\}. \quad \text{(C3)}$$

Using the explicit form of $W_{mn}^{(\rm e)}$, Eq. (A3), one can show that $a_n > 0$.

1. Temperature range $\bar{n} \gg \lambda^3$

In this section we analyze the change Δ_n of the eikonal of the probability distribution for $1 \gg \bar{n} \gg \lambda^3$. As we will see, in contrast to the range $\bar{n} \ll \lambda^3$ discussed in the main text, for $\bar{n} \gg \lambda^3$ the dominating term in $\varkappa_n$ is $\varkappa_n'$. It describes the contribution from transitions from not too strongly separated states. From Eq. (11), the leading-order term in Δ_n in the range $n - n_\varkappa \gg \bar{n}^{-1/3}$ is still given by Eq, (12). However, when calculating $\varkappa_n'$ one should add a correction $-(n-m)\epsilon_n$ to the leading term in $(\Delta_n - \Delta_m)/\lambda$, with $|\epsilon_n| \ll 1$. This is reminiscent of the calculation of the correction to the eikonal for a parametric oscillator [11], which was done, however, away from the crossover region.

From Eq. (11) of the main text, the sum over m in $\varkappa_n'$ is a second derivative with respect to ϵ_n of a geometric series, since the prefactor in $w_{mn}^{(0)}$ is $C^{(w)}(g_m, g_n) \propto (g_m - g_n)^2 \propto (n-m)^2$ for $|n-m| \ll 1/\lambda$; see Eq. (C1). Then

$$\varkappa_n' \approx \left(\bar{n}/\epsilon_n^3\right) C_\varkappa(g_n), \quad C_\varkappa(g_n) = 8\nu_n^4 \kappa \big/ \lambda\beta W_n^{(\mathrm{e})}. \tag{C4}$$

The coefficient $C_\varkappa(g)$ is independent of λ and is ~ 1, generally. Since $\varkappa_n' \lesssim 1$, from Eq. (C4) we have $\epsilon_n \sim \bar{n}^{1/3}$, and

$$\Delta_n \approx -\int_{g_n}^{g_\varkappa} dg f(g) - \bar{n}^{1/3} \int_{g_n}^{g_\varkappa} dg \nu^{-1}(g) C_\varkappa^{1/3}(g), \quad n - n_\varkappa \gg 1. \tag{C5}$$

The correction $\propto \bar{n}^{1/3}$ in Eq. (C5) increases $|\ln \rho_n|$ by a term $\propto \bar{n}^{1/3}/\lambda \gg 1$. Respectively, $\varkappa_n''$ as given by Eq. (11) becomes exponentially small, in agreement with the assumption that it could be disregarded. On the whole, as the ratio $\bar{n}^{1/3}/\lambda$ changes from small to large, so also does the ratio $\varkappa_n'/\varkappa_n''$, starting from large n.

From Eq. (C1) and from Eq. (8), for $\bar{n}$ approaching $\lambda^{3/2} \ll 1$ the quasienergy $g_\varkappa$ approaches g_e. For $\bar{n} \gg \lambda^{3/2}$, i.e., outside the crossover region, $T > T_{c2}$, the rates of transitions into all states with $g_n < g_e$ are determined by absorption (thermal) processes. In this range $\varkappa_n = \varkappa_n'$, and the eikonal $R_n = R_n^{(0)} + \Delta_n$ is determined by Eq. (C5). For $\bar{n} \gg \lambda^3$ the slope $d|\ln W_{\mathrm{sw}}|/dT^{-1} \propto (\hbar\omega_0/k_B)\bar{n}^{1/3}/\lambda$ is much larger than in the region of the plateau, where it is equal to $\hbar\omega_0/k_B$.

[1] *Fluctuating Nonlinear Oscillators: from Nanomechanics to Quantum Superconducting Circuits*, edited by M. I. Dykman (Oxford University Press, Oxford, 2012).

[2] R. Vijay, M. H. Devoret, and I. Siddiqi, Rev. Sci. Instrum. **80**, 111101 (2009); K. W. Murch, R. Vijay, I. Barth, O. Naaman, J. Aumentado, L. Friedland, and I. Siddiqi, Nat. Phys. **7**, 105 (2011).

[3] V. Peano and M. Thorwart, Phys. Rev. B **70**, 235401 (2004); Europhys. Lett. **89**, 17008 (2010).

[4] I. Serban and F. K. Wilhelm, Phys. Rev. Lett. **99**, 137001 (2007).

[5] F. Mallet, F. R. Ong, A. Palacios-Laloy, F. Nguyen, P. Bertet, D. Vion, and D. Esteve, Nat. Phys. **5**, 791 (2009); F. R. Ong, M. Boissonneault, F. Mallet, A. C. Doherty, A. Blais, D. Vion, D. Esteve, and P. Bertet, Phys. Rev. Lett. **110**, 047001 (2013).

[6] L. S. Bishop, E. Ginossar, and S. M. Girvin, Phys. Rev. Lett. **105**, 100505 (2010).

[7] A. Verso and J. Ankerhold, Phys. Rev. E **82**, 051116 (2010).

[8] C. M. Wilson, T. Duty, M. Sandberg, F. Persson, V. Shumeiko, and P. Delsing, Phys. Rev. Lett. **105**, 233907 (2010).

[9] P. D. Nation, J. R. Johansson, M. P. Blencowe, and F. Nori, Rev. Mod. Phys. **84**, 1 (2012).

[10] M. I. Dykman and V. N. Smelyanskii, Zh. Eksp. Teor. Fiz. **94**, 61 (1988).

[11] M. Marthaler and M. I. Dykman, Phys. Rev. A **73**, 042108 (2006).

[12] H. Kramers, Physica (Utrecht) **7**, 284 (1940).

[13] I. Affleck, Phys. Rev. Lett. **46**, 388 (1981).

[14] A. I. Larkin and Y. N. Ovchinnikov, JETP Lett. **37**, 382 (1983).

[15] P. D. Drummond and D. F. Walls, J. Phys. A **13**, 725 (1980); H. Risken, C. Savage, F. Haake, and D. F. Walls, Phys. Rev. A **35**, 1729 (1987).

[16] H. Touchette, Phys. Rep. **478**, 1 (2009).

[17] A. Kamenev, *Field Theory of Non-Equilibrium Systems* (Cambridge University Press, Cambridge, 2011).

[18] M. Khasin and M. I. Dykman, Phys. Rev. Lett. **103**, 068101 (2009).

[19] G. J. Walls and D. F. & Milburn, *Quantum Optics* (Springer, Berlin, 2008).

[20] V. Peano, M. Marthaler, and M. I. Dykman, Phys. Rev. Lett. **109**, 090401 (2012).

[21] L. Mandel and E. Wolf, *Optical Coherence and Quantum Optics* (Cambridge University Press, Cambridge, 1995).

[22] M. I. Dykman and M. A. Krivoglaz, in *Soviet Physics Reviews*, edited by I. M. Khalatnikov (Harwood Academic, New York, 1984), Vol. 5, p. 265.

[23] D. N. Zubarev, Sov. Phys. Usp. **3**, 320 (1960).

[24] L. D. Landau and E. M. Lifshitz, *Quantum Mechanics: Non-Relativistic Theory*, 3rd ed. (Butterworth-Heinemann, Oxford, 1997).